

# Generic Representation Learning for Dynamic Social Interaction

Yanbang Wang  
ywangdr@cs.stanford.edu  
Stanford University

Pan Li  
panli@purdue.edu  
Stanford University, Purdue  
University

Chongyang Bai  
cy@cs.dartmouth.edu  
Dartmouth College

V.S. Subrahmanian  
vs@dartmouth.edu  
Dartmouth College

Jure Leskovec  
jure@cs.stanford.edu  
Stanford University

## ABSTRACT

Social interactions, such as eye contact, speaking and listening, are ubiquitous in our life and carry important clues of human’s social status and psychological state. With evolving dynamics fundamentally different from social relationships, the complex interactions among a group of people are another informative resource to analyze patterns of social behaviors and characteristics. Despite the great importance, previous approaches on extracting patterns from such dynamic social interactions are still underdeveloped and overly task-specific. We fill this gap by proposing a *temporal network* formulation of the problem, together with a representation learning framework, temporal network-diffusion convolution networks (TNDN). The framework accommodates the many downstream tasks with a unified structure: we creatively propagate people’s fast-changing descriptive traits among their evolving *gazing networks* with specially designed (1) network diffusion scheme and (2) hierarchical pooling to learn high-quality embeddings for downstream tasks using a consistent structure and minimal feature engineering. Analysis show that (1) can not only capture patterns from *existed interactions* but also people’s *avoidance of interactions* that turn out just as critical. (2) allows us to flexibly collect different fine-grained critical interaction features scattered over an extremely long time span, which is also key to success while it empirically fails almost all the previous temporal GNNs based on recurrent structures. We evaluate our model over three different prediction tasks, detecting deception, dominance and nervousness. Our model not only consistently outperforms previous baselines but also provides good interpretation by implying two important pieces of social insight derived from the learned coefficients.

## ACM Reference Format:

Yanbang Wang, Pan Li, Chongyang Bai, V.S. Subrahmanian, and Jure Leskovec. 2020. Generic Representation Learning for Dynamic Social Interaction. In *Proceedings of KDD ’20: Knowledge Discovery in Databases (KDD MLG’20)*. ACM, New York, NY, USA, 9 pages. <https://doi.org/10.1145/nnnnnnn.nnnnnnn>

Permission to make digital or hard copies of all or part of this work for personal or classroom use is granted without fee provided that copies are not made or distributed for profit or commercial advantage and that copies bear this notice and the full citation on the first page. Copyrights for components of this work owned by others than ACM must be honored. Abstracting with credit is permitted. To copy otherwise, or republish, to post on servers or to redistribute to lists, requires prior specific permission and/or a fee. Request permissions from [permissions@acm.org](mailto:permissions@acm.org).

KDD MLG’20, Aug 24–27, 2020, San Diego, CA

© 2020 Association for Computing Machinery.

ACM ISBN 978-x-xxxx-xxxx-x/YY/MM... \$15.00

<https://doi.org/10.1145/nnnnnnn.nnnnnnn>

## 1 INTRODUCTION

Social interactions, referring to numerous and complicated actions among two or more people, have woven themselves into every piece of our daily life [33]. They are one of the most ubiquitous forms that people connect with each other, and can happen whenever several people meet physically or online with video meeting tools. Such interactions, featured by synchronously occurred high-frequency eye contacts, fast-changing facial expressions, voice features and even physical proximity, have evolving dynamics fundamentally different from acquaintance-based social networks.

With such informative signals that characterize complex human group behaviors, psychological state and social-economic status, social interactions become critical data resources for social scientists to study patterns of human behaviors and make further inferences [25]. For example, where, when and how people interact with others may provide informative cues to solve various social tasks including deception detection [4, 13], dominance identification [5, 8], personality traits characterization [30] and friendship inference [16].

However, we recognize that existing literature [4, 5, 8, 14, 15, 41] on each of these tasks primarily rely on handcrafted features that are hardly transferable to each other. This makes the modeling process overly task-specific and high-demanding for domain expertise. In that regard, we propose a more generic framework that formulates social interactions with such vigorous dynamics by a temporal network for more unified representation learning. Central to this prototype is the usage of people’s evolving eye-gazing or speak-and-listen-to relationships for temporal network construction. With eye contacts as the key to signal information flows [36] in a social interaction, both the explicit messages and people’s underlying influence on each other can now be naturally modeled into a *graph diffusion* process, which essentially instantiates a variant of the powerful (temporal) graph neural network [23]. We term this temporal network model *dynamic social interaction network*.

There are several temporal GNN frameworks proposed recently for representation of generic temporal networks. However, they are not well-suited to our downstream tasks. One important reason is that they are primarily designed to *fit* the occurrence/attributes of temporal edges and thus almost always place an imbalanced weight on events towards the sequence’s end [11, 29, 39, 47]. However, our tasks (deception detection for example) essentially need to *collect* the different, sporadic and potentially overlapping traits of communication throughout the interaction. Such mismatch becomes especially noticeable with long, fine-grained interaction sequence

(which is a must due to the event’s high-frequency nature): a 6-minute conversation extracted on 3 FPS yields more than 1000 snapshots which fails all the previous temporal models based on recurrent structures [20, 21, 28, 35, 37]. Some others either assume a static underlying graph structure, such as those designed for traffic forecasting [26, 45], or claim to be able to handle dynamic node attributes but have never been evaluated over the case with highly dynamic node attributes as those in social interaction networks [21, 28, 35, 37].

Our contribution in this paper is summarized as the following:

- We propose the formulation of social interactions into a temporal network prototype to enable unified representation learning for the many downstream tasks with minimal level of knowledge-based feature engineering.
- we propose an end-to-end neural-network-based model, *temporal network-diffusion convolution networks* (TNDCN) that both intuitively model the information flow with enhanced graph convolution and flexibly collect scattered fine-grained patterns over long time with special hierarchical pooling.
- We evaluate TNDCN over three different social tasks including deception, dominance and nervousness detection. Our model consistently outperforms a variety of our baselines. In-depth analysis shows that the learnt coefficients further yield interesting insights on interaction patterns.

## 2 PROBLEM FORMULATION

In this section, we first introduce notations of static graphs in general. Then, we introduce our problem into the context by further formulating it into the prototype of temporal graphs. We use capital letters  $N, M, M'$  to denote some positive integers.

### 2.1 General Graph Notations

A static network can be represented as a graph  $G = (V, E)$  where  $V$  denotes the set of nodes and  $E$  the set of edges.  $N = |V|$ . Networks that we discuss include both directed and undirected. As an undirected graph can be viewed as a special case of directed one, we assume  $G$  is directed hereafter unless specified.

Graph  $G$  is associated with adjacency matrix  $A \in \mathbb{R}^{N \times N}$  where  $A_{uv} = 1$  if and only if  $(u, v) \in E$ . Also, we define the diagonal out-degree matrix  $D_{\text{out}} \in \mathbb{R}^{N \times N}$  where its  $u$ -th diagonal component is  $d_{\text{out},u} = \sum_{v \in V} A_{uv}$ . The random walk matrix over  $G$  is defined as

$$W = D_{\text{out}}^{-1}A. \quad (1)$$

### 2.2 Dynamic Social Interaction Networks

Central to the prototype’s formulation are two things: nodes, which represent people, and timestamped edges, which represent interactions between two people and are usually mapped from people’s evolving eye-gazing or speak-listen relationships. Dynamic personal traits are further associated with nodes and communication-based properties like gazing probabilities are associated to edges.

To record social interactions, the most common practice is to leverage a variety of sensors to record snapshots of interaction scenes of high time resolution. Therefore, we define our data structures using *temporal graph snapshots*:  $\{G_t\}_{1 \leq t \leq T}$  where  $G_t = \{V_t, E_t\}$ . We further denote the universal node set  $V = \bigcup V_t, \forall t \in [1, T]$ , so that  $V$  is fixed across different snapshots.

As mentioned, dynamic social interaction networks can be associated with both dynamic node and/or edge attributes. and dynamic edge attributes. For node attributes, we have  $\{X_t\}_{1 \leq t \leq T}$ , where the row of  $X_t$  corresponding to node  $u$ ’s initial attributes. For edges, we also allow the network edge associated with a quantified attribute, denoted by a weighted adjacency matrix  $A$  in generalized form. For example, an edge can carry the likelihood of one person looking at the other, or the wireless signal strength that one’s smart device receives from the other’s. Generalization to multi-type edges yields multi-view temporal network, which beyond our discussion of this work and left for future work. Note that our definition allows both edge and node attributes to evolve dynamically though.

Our goal is to learn representations for nodes in these networks that capture important patterns from their social interaction behaviors. Once the representations are learned, prediction/inference for certain tasks can be accomplished by feeding these representations into inference blocks for downstream tasks. We claim our approach can be used for general node-level prediction tasks that require patterns to be extracted from dynamic social interaction networks. We demonstrate this capability by considering the following three tasks: detection lying people, dominant people, and nervous people in a social interaction event. The specific inference blocks and training objectives will be specified in Section 5.

## 3 PROPOSED MODEL

Our model temporal network-diffusion convolutional network (TNDCN) consists of two main components, *Network Diffusion* of node attributes, and Set-Temporal Convolution-based *hierarchical pooling* over time, as shown in Figure 1. The obtained node embeddings will be further fed into a simple task-driven output block to either compute loss (during training) or make inference. The loss is specified by tasks so we introduce it in Section 5.

### 3.1 Network Diffusion Component

We propose using *network diffusion process* to most intuitively model the information flows carried by interactive behaviors in our dynamic network: given people’s personal traits in a certain snapshot quantified by node attributes  $X^{(0)} \in \mathbb{R}^{N \times M}$ , the  $k$ -hop network diffusion can be written as

$$X^{(k)} = (W^T)^k X^{(0)} \quad (2)$$

where  $W^T$  is the transpose of  $W$ . This process is further enhanced by two sets of parameters:

**Parameters  $\beta$  for making or avoiding interactions.** One speciality of social interaction networks is that the behavior to avoid interactions could be very informative. For example, deceivers tend to avoid gazing at others [32], and some deceivers may tend to be abnormally quiet in front of others [41] due to their low-level self-confidence. However, different phenomena could happen between a follower and his leader [42]. So we consider graphs corresponding to the original interaction networks and their complement graphs simultaneously. Concretely, for each type of interaction network with adjacency matrix  $A$ <sup>1</sup>, we also consider the corresponding adjacency matrix of the complement network  $\bar{A} = I - A$  where  $I$  is the

<sup>1</sup>We assume the components of  $A$  are normalized within interval  $[0, 1]$ .

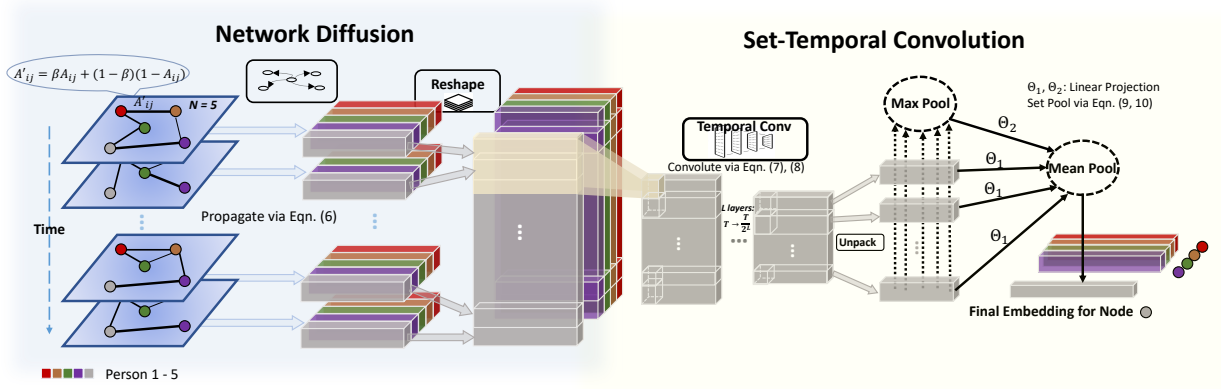


Figure 1: Temporal Network-Diffusion Convolution Network: an Illustration.

identity matrix. Then, we introduce another parameter  $\beta \in [0, 1]$  to merge these two networks to obtain a new adjacency matrix via

$$A' = \beta A + (1 - \beta)\bar{A} = (2\beta - I)A + (1 - \beta)I. \quad (3)$$

Apparently, this parameter  $\beta$  have physical implication. A greater  $\beta$  suggests making interaction is more informative to the prediction task, while a smaller  $\beta$  emphasizes that avoiding interaction may be the key clue. From now on, we will diffuse node attributes over the random walk matrix derived from this parameterized network  $A'$  based on (1), i.e., replace  $W$  in Eqn. 2 by  $W' = D'^{-1}A'$ . Admittedly, using graph would lead to a densely connected network which can lead to large computation cost in large graphs. However, this issue would not appear here since dynamic social interactions in our context can hardly involve people of more than hundreds in a single interaction event.

**Parameter  $\Gamma_k$  for different-hop interactions.** The model is now to perform different-step network diffusion. By assigning a group of learnable parameters  $\{\Gamma_k\}_{k \geq 0}$ , where  $\Gamma_k$  is a diagonal matrix for the hop  $k$ , we consider the transformation of initial node attributes  $X^{(0)} \in \mathbb{R}^{N \times M}$  based on network diffusion as

$$H = \sum_{k \geq 0} H^{(k)} \Gamma_k = \sum_{k \geq 0} (W'^T)^k H^{(0)} \Gamma_k, \quad H^{(0)} = f(X^{(0)}) \quad (4)$$

where  $f(\cdot) : \mathbb{R}^{N \times M} \rightarrow \mathbb{R}^{N \times M'}$  could be as simple as identity mapping ( $M' = M$ ) or as complex as multi-layer perceptrons (MLP) that properly transform and normalize initial node attributes. Here,  $M'$  is the dimension of output channel.  $\Gamma_k \in \mathbb{R}^{M' \times M'}$  provides the weights for the  $k$ -hop diffusion. The corresponding  $q$ -th diagonal component, denoted by  $\gamma_{k,q}$ , is the weight for  $q$ 's output channel. In practice, typically only the first several hops could be informative so we may set an upper bound to the number of hops: 5 ~ 10 steps provide good enough results in practice.

Note that the formulation (4) has many implications. Consider the sequence  $\{\gamma_{k,q}\}_{k \geq 0}$  for any  $q$  and suppose  $f$  is identity mapping. From the perspective of graph spectral convolution,  $\{\gamma_{k,q}\}_{k \geq 0}$  corresponds to weights on different levels of the smoothness of  $q$ -th node attributes. Moreover, different fixed formulations of  $\gamma_{k,q}$  also provide different types of ranks of nodes:  $\gamma_{k,q} \propto \alpha^k$  corresponds to PageRank [31];  $\gamma_{k,q} \propto \frac{h^k}{k!}$  corresponds to heat-kernel PageRank [10]. Extensive feature engineering shows that different

formulations of ranks could be important signals to detect deceivers or leaders among group of people [4, 5]. Our formulation based on learnable parameters allows for more representation power to cover multiple prediction tasks. Moreover, for model interpretation, as  $W'^T$  is column stochastic, it will keep the  $\ell_1$ -norm of every column of  $H^{(k)}$  unchanged (with non-negative features) and thus naturally hold normalizing property. Therefore, the value  $|\gamma_{k,q}|$  and the sign of  $\gamma_{k,q}$  are naturally interpreted as the effect of  $k$ -hop diffusion of  $q$ -th node attribute to the final representation. Even when we choose  $f$  as MLP, decoupling parameters  $\Gamma_k$  on diffusion and parameters on pure transformation of node attributes in  $f(\cdot)$  keeps the effect of network diffusion distinguishable, which is useful for model interpretation.

Note that there could be variants of (4) to further increase model complexity and representation power. By adding nonlinear transformation of each step  $H^{(k)}$  before letting it propagate, one may get the model of graph convolution networks [23]. However, adding non-linearity per step increases the difficulty for training, which limits the steps of propagation to 2-3, and could simultaneously hurt the interpretation of models. As our experiments do not show any improvement based on non-linearity, a simpler model is preferred. Similar gain by removing non-linearity has also been observed in many recent literatures on graph neural networks [24, 43]. However, to the best of our knowledge, we are the first to show the success of this manner to process dynamic networks.

### 3.2 Set-Temporal Convolution Component

To aggregate node features over time, we propose a method called Set TCN (S-TCN) to handle the complex and long-term temporal social interactions. As mentioned, there are two challenges in designing the block: being able to handle an extremely long sequence of snapshots because of the high time resolution, and being able to capture local dynamics typically subtle and scattered randomly in the whole time span. Correspondingly, our S-TCN block consists of two components: multi-layer temporal convolution and set pooling.

**Multi-layer Temporal Convolution.** The input of this block is a sequence of node features  $\{H_t\}_{1 \leq t \leq T}$  where  $H_t \in \mathbb{R}^{N \times M}$  denotes the node features for each snapshot  $t$  obtained via (4). The  $l$ -th

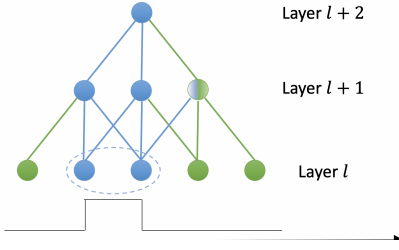


**Figure 2: Receptive field of temporal convolution: The interaction happened at the two blue timestamps in layer  $l$  is captured by the blue timestamps in layers  $l+1$  and  $l+2$  through convolution operation.**

temporal convolution layer is defined as the following:

$$\begin{aligned} Z_t^{(0)} &= H_t \\ \bar{Z}_t^{(l)} &= \text{ReLu}(Z_t^{(l-1)} * C_t^{(l)}) = \text{ReLu}\left(\sum_{\tau \in [1, w]} X_{t-\tau+1} C_\tau\right) \\ Z_t^{(l)} &= \text{max-pooling}(\{\bar{Z}_{2t}^{(l)}, \bar{Z}_{2t+1}^{(l)}\}), \quad \text{for } 1 \leq l \leq L \end{aligned}$$

where  $*$  is the convolution operator,  $\{C_\tau^{(l)}\}_{1 \leq \tau \leq w}$  is the convolution kernel,  $w$  is window size.

The number of layers  $L$  typically depends on the time-scale of interactions we want to extract patterns from. It is related to the receptive field of convolution networks (See Fig. 2)). The success of TCN in our setting may be due to its clear and flexible receptive fields. If the size of max-pooling kernel is 2 as what we use in the equation, then neurons in the last ( $L$ -th) convolution layer can perceive the signals with length  $2^L$ . The size of receptive field can be set based on two important usage: (1) Signal Denoising. convolution kernels are widely known for their capability to function as low-pass filters. By stacking different numbers of convolution layers, we can explicitly tune the capability of the network for signal smoothing; (2) Temporal feature extraction from well-defined "locality". By tuning the number of layers, one can actively search for the optimal receptive field length to gather meaningful features. Such length is also an important reference for us to understand people's interaction.

Given a proper depth of TCN  $L \in [2, 4]$  to obtain a proper size of receptive field, the length of the final layer could be very long ( $\geq 50$ ), because the original time series  $T \gtrsim 1000$  is long.

**Set Pooling.** As opposed to online social networks that often show seasonal patterns, there are seldom periodical patterns in offline social interaction networks. Consider eye contact in conversation/meeting among a group of people. Informative patterns of interactive behaviors of people are usually randomly scattered in the long time span. Therefore, based on the local patterns captured by TCN, we use set pooling over the obtained sequence  $\{Z_t^{(L)}\}_{1 \leq t \leq T^{(L)}}$  to extract the message scattered within this long sequence. We observe that the following form is generally effective across different applications: First, we impose max pooling (5) on  $\{Z_t^{(L)}\}_{1 \leq t \leq T^{(L)}}$  to emphasize the critical local patterns; Then, we linearly merge the output of max pooling into each  $Z_t^{(L)}$  to let each  $Z_t^{(L)}$  capture global information; Finally, after a simple ReLu activation, we obtain the

output via mean pooling.

$$Z_{\max} = \text{max-pooling}_{1 \leq t \leq T^{(L)}}(Z_t^{(L)}), \quad Z_t' = Z_t^{(L)} \quad (5)$$

$$Z_{\text{out}} = \text{mean-pooling}_{1 \leq t \leq T^{(L)}}(\text{ReLu}(\Theta_1 Z_t' + \Theta_2 Z_{\max})) \quad (6)$$

Note that the max pooling captures the essence of randomly scattered patterns while the second step based on linear combination and the mean pooling is found out to be useful to improve the robustness of feature aggregation. Note that this set-pooling technique properly tailors Deep Sets [46] for our setting.

## 4 RELATED WORK

The research related to our problem spans two broad areas:

**Methods to Analyze Social Interactions.** Lots of research has been conducted to identify human behaviors and relationship during social interactions such as leadership [8], dominance [5, 22], friendship [9], and deception [4, 14]. These works focus on designing task-specific features in short periods and aggregate them to long-term feature vectors via statistical methods. The obtained features are then fed into standard classifiers (e.g. SVM, Random Forest). These engineered features, although shown to be powerful in their corresponding tasks, are less general and often requires specific domain knowledge in social science and psychology theories (e.g. visual dominance ratio [15], emotions and deception [41]). Moreover, the hand-crafted features become more noisy when building upon raw features. To effectively aggregate features over the long temporal domain, extensive statistical methods are employed such as summation, median and variance [8, 14], histograms and bag-of-words [4, 5]. These indifferentiable aggregations make potential models untrainable. In contrast, due to our neural-network-based module, we obtain a differentiable model that connects raw networks directly to the social tasks and allows for an end-to-end training. By taking advantage of this training procedure, the model naturally learns the effect of interacting networks for various social tasks without using extensive statistical analysis.

**Representation Learning for Dynamic Networks.** The success of representation learning for dynamic social interaction networks strongly depends on processing the interweaving high-dynamic node attributes and interactions. So we first partition previous approaches to learn representation of dynamic networks into two categories regarding whether dynamic node attributes can be processed. We do not provide a detailed review of works unable to take dynamic node attributes including [1, 11, 20, 29, 38, 39, 47, 48]. Works that were claimed to digest dynamic node attributes all work on networks snapshots [21, 28, 35, 37]. They generally follow the pipeline by first propagating node attributes of each network snapshot and then aggregating them over time. Works [21, 28, 37] use graph convolution networks [23] for the first step while Sankar et al. [35] leverages graph attention networks [40]. For the second step, works [21, 28, 37] use RNN and its variants to aggregate node representations, while Sankar et al. [35] uses self-attention mechanism. However, all these approaches share the issue of limited memory capacity when #snapshots  $> 100$ . Moreover, despite proposed to process dynamic node attributes, they have not been evaluated in the setting with highly dynamic node attributes as those in dynamic social interaction networks.

## 5 EMPIRICAL STUDY

### 5.1 Experiment Settings

**Overview.** Our proposed model is evaluated on three different node-level prediction social tasks over 4 datasets:

- (1) Dominance Detection: RESISTANCE-1 [6], ELEA [34];
- (2) Deception Detection: RESISTANCE-2 [6];
- (3) Nervousness Detection: RESISTANCE-3 [6];

Task (1) and (3) aims to identify the *most* dominant/nervous person in a social interaction event happening between 3-8 people. Task (2) aims to detect all the hidden liars in a social interaction event happening between 5-8 people. Therefore, we consider Task (1), (3) as a one-vs-rest classification problem, and consider Task (2) as a binary classification problem.

In its original format, each dataset is a collection of videos. Each video records a conversation whose duration ranges from around 5 to 30 minutes, with different conversation contexts, which we will introduce slightly afterwards. We preprocess each video using vision-based and audio-based techniques of various sources, which for each conversation generates around 800-4500 dynamic network snapshots (on 3 FPS, as described in Section 2.2). In the rest of this section, we will explain the dataset background, ground-truth label collection, feature preprocessing, as well as other implementation details including baselines and model tuning.

**Dataset: RESISTANCE-1, 2, 3.** All three dataset are a collection of videos and surveys recording people’s performance in a role-playing party game called the Resistance: Avalon. Each game has 5 to 8 players secretly split into two rivaling teams before the game starts: the resistance team (“good” people, Team A, accounting for about 70%) and the spy team (“bad” people, Team B, the rest 30%). Team B know everyone’s real identity but Team A do not. Both teams’ goal is to beat each other in the “missions” conducted by discussion and election, which involves frequent deception behavior (presumably only from Team B) and argument, query and persuasion (from all parties). In order to persuade, very often people tend to be dominant and avoid appearing nervous, Please see supplementary material<sup>2</sup> for more background. The three dataset share about 50% videos in common while for the rest they each differ slightly due to several practical reasons such as label missing or mismatch.

Labels for RESISTANCE-1, 3 are generated by referencing surveys taken by all participants after each game. The surveys take the form of questionnaires, asking each participant to rate the dominance and nervous level of the other people. We treat the median score of each person (rated by others) as its ground truth score, ties broken by further comparing the mean. Labels for RESISTANCE-2, which are Team A & B’s identity of each game, are given by the dataset. Considering the gaming rules, it is presumable that Team B (spies) are essentially lying throughout the game.

**Dataset: ELEA** The dataset [34] is a widely used benchmark for modeling and detecting personal traits such as dominance [5]. The dataset can be accessed here<sup>3</sup>. In each video, 3-4 participants collaboratively performed a “winter survival task” by having peaceful discussions. We perform dominance detection task on the dataset as other labels are unavailable

<sup>2</sup>Supplementary material: <https://bit.ly/36ipjoO>

<sup>3</sup>ELEA dataset: <https://www.idiap.ch/dataset/elea>

Labels are generated in a slightly different way following the protocols of [2, 5]: we are detecting *more* dominant people instead of *the most*. This also provides a new angle of evaluation. There are two categories of dominance scores: (1) perceived dominance (PDom), which is scores rated by the game organizers who hosted and monitored the game; (2) ranked dominance (RDom), which is scores rated by game participants to each other. we assign binary dominance labels to people by thresholding their dominance scores by the median values of people in each video.

**Feature Extraction.** We extract the following social interaction features from videos on frequency of 3 FPS using a combination of toolkit:

- (1) Emotion: intensity of eight emotions + two facial traits (smile, open eyes) by Amazon Recognition;
- (2) FAU: intensity of 17 facial action units using OpenFace [7];
- (3) MFCC: voice features widely used in audio analysis [12];
- (4) Speak Prob.: Probability a person is speaking estimated from lip movement [17];
- (5) Gazing Prob.: probability that each person looks at each other players estimated from eye movement [3]. For each person his Gazing Prob. towards other people sums up to 1.

Our dynamic social interaction network is constructed from the last feature.

**Output Layer & Loss.** As mentioned, we consider Task (2) a binary classification problem, so the output block for processing each person’s representation is a simple logistic regression instantiated by a densely connected neural network layer plus the Sigmoid nonlinearity.

For task (1) and (3) to select one out of a set 3-8 representations we further use the following transformation: Let  $Z_{out} \in \mathbb{R}^{N \times e}$  taken from Eqn. 6 be the learned representation of all the people in one interaction event, where  $N \in [3, 8]$  is the number of people and  $e$  is the representation length). The  $i$ -th people’s output logit is given by:

$$Z_i = Z_i W_1 + \text{Mean-pooling}(\{Z_i\}_{1 \leq i \leq N}) W_2, \quad \text{for } 1 \leq i \leq N \quad (7)$$

$$\hat{Y} = \text{softmax}(Z W_3) \quad (8)$$

where  $W_1, W_2 \in \mathbb{R}^{e \times e}$  and  $W_3 \in \mathbb{R}^{e \times 1}$  are projection matrices whose parameters are to be learned. We use cross entropy loss for all tasks and back-propagate the errors to all aforementioned learnable parameters for optimization.

**Baselines.** Our framework is compared with two sets of baselines. The first set is task-specific baselines proposed uniquely for each task:

- Dominance Detection: MKL [8], which is based on hand-crafted features like voice pitch and speaking rate; two versions of the GDP [5] which primarily relies on their hand-crafted feature called DomRank: GDP with random forest classifier (GDP-RF), and GDP with multi-layer perceptron classifier (GDP-MLP); DELF [5] also uses DomRank.
- Deception Detection: ADD [44] based on handcrafted micro facial expression and NLP features; TGCN-L [27] based on gazing probabilities, and LiarRank [4] based on all the features we used but aggregating them in a special manner;

Task No. and Task	Dataset	Dynamic Network Sequences	Time Steps (Avg.)	Nodes	Interactions <sup>†</sup>
(1) Dominance Identification	RESISTANCE-1	956	2,514	4780	$4.007 \times 10^6$
(1) Dominance Identification	ELEA	21	1,350	84	$6.474 \times 10^3$
(2) Deception Detection	RESISTANCE-2	2,157	1,800	10,785	$2.439 \times 10^7$
(3) Nervousness Detection	RESISTANCE-3	1,097	1,800	5,485	$4.910 \times 10^7$

<sup>†</sup> We count all the interactions with gazing probability  $\geq 0.5$ .

**Table 1: General statistics of the dynamic networks used for representation learning.**

- Nervousness Detection: Facial Cues [19] based on facial action units, Random Forest and Logistic Regression<sup>4</sup>;

In addition, to ensure fair comparison, we further pick for each task the best reported baseline to further evaluate them on other tasks. Furthermore, We add one more generic temporal GNN-based model was SOTA on sequence modeling: GCN-LSTM [37]. It combines graph convolutional network with LSTM. For more details on features and aggregation schemes used by each baseline, please see our supplementary material.

**Model training.** Following protocols of most baselines, we randomly partition the total number of dynamic social interaction networks in each dataset into 10 folds. Each time, a different 10% is reserved for testing, and the rest for training. We use cross-entropy loss and Adam optimizer to train our TNDN model. Hyperparameters are determined using grid search and their detailed values are provided in supplementary material. The whole pipeline is implemented in PyTorch. Following protocols of most previous work, we report the average accuracy on test set by running the pipeline for 10 times using different random seed to initialize parameters.

## 5.2 Performance Comparison

Table 2 compares performance of our model and other baselines on the three tasks. It shows that our model significantly outperforms the strongest baselines in Task 2,3 and also achieves comparable result with the strongest baseline on Task 1. Notice that our best model achieves this with less than one-fifth parameters of DELF and GDP. We also notice that our model has more significant gain in the challenging tasks 2 and 3. The two tasks are challenging essentially because they are both probing for something that the interaction participants are purposely concealing. For such cases we explain that effectively capturing the temporal cues is the key to success. While almost all the baselines come with proper graph convolution or careful feature engineering work, their processing of temporal information falls insufficient, either mean pooling (TGCN, Logistic., Random F.), Fisher Vector encoding (FacialCues), histogram encoding (DELF), or many-to-one LSTM (GCN-LSTM). Also notice the GCN-LSTM’s failure on most tasks, which shows the insufficiency of temporal sequence modeling techniques based on recurrent structures.

<sup>4</sup>Since very little previous literature exists on this task, we further implement two baselines that use a simple classifier to process all our input features independently, i.e. without any network-level operation

## 5.3 Model Interpretation

The linearity of parameters in network diffusion provides model interpretation. Next, we investigate these parameters and explain the induced social insights.

**Interpretation I: Balancing Weight  $\beta$ .** Recall from Section 3.1 that  $\beta$  is the learnable parameter that directly controls the relative importance of proactive interaction versus avoidance of interaction. Figure 3 displays how the  $\beta$  converges during the training (initialized to 0.5, i.e. neutral). For each task we ran multiple times

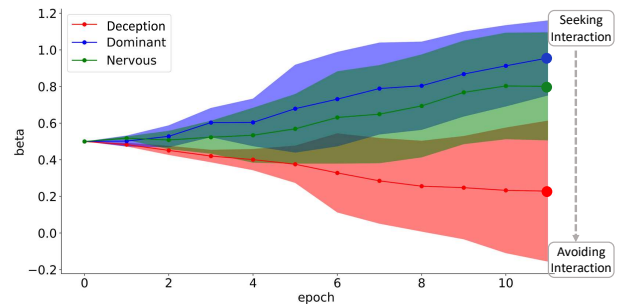


**Figure 3: Different convergence behaviors of  $\beta$  during training, 95% confidence intervals shaded. Trained on RESISTANCE-1,2,3 respectively.**

by introducing small perturbation to  $\beta$ ’s initialization. The figure shows that the parameter exhibits very different convergence behavior across different tasks. In particular, the deception detection task  $\beta$  significantly drops to around 0.2, which indicates that avoidance of interaction may be much more important than contacts in detecting deception. Interestingly, this phenomenon coincides with findings from a psychological study [32] on eye movement of people in various contexts. It is also quite understandable that dominant people are more easily identified with their aggressive way of reaching out to people (rather than escape to do so). Nervous people, on the other hand, seem to be identified with a mixture of the two extremes. The analysis on  $\beta$  shows its prediction power and high value to understanding human’s avoidance of social interactions.

**Interpretation II: Diffusion Weights  $\{\Gamma_k\}$ .** Recall from Equation 4 that  $\{\Gamma_k\}_{0 \leq k \leq K}$  is a sequence of diagonal matrices where  $\Gamma_k \in \mathbb{R}^{M' \times M'}$  contains the weights corresponding to  $M'$  features’  $k$ -hop diffusion. Therefore, when we finish training we would obtain  $K + 1$  diffusion weights for each of the  $M'$  features. Analyzing these diffusion weights provides us with important insights of how the interaction network actually helps shape the original features during the diffusion. Fig. 4 displays such weights for four of the features’ (here diffusion steps  $K = 10$ ) after being trained on the nervousness

Group \ Task	Dominance-R*		Dominance-E*		Deception		Nervousness	
Task-specific Baselines	MKL	0.879	Aran et al.	0.657/0.598	FAU	0.608	R. Forest	0.678
	GDP-MLP	0.917	Okada et al.	0.677/0.686	TGCN-L	0.550	Logistic	0.493
	GDP-RF	0.878	Humans	0.686/-	ADD	0.632	-	-
"Universal" Baselines†	DELf	0.889	DELf	0.765/0.677	DELf	0.641	DELf	0.721
	LiarRank	0.827	LiarRank	0.674/0.612	LiarRank	0.665	LiarRank	0.731
	FacialCues	0.746	FacialCues	0.702/0.665	FacialCues	0.591	FacialCues	0.733
	GCN-LSTM	0.821	GCN-LSTM	0.732/0.585	GCN-LSTM	0.562	GCN-LSTM	0.629
Ours	TNDCN	0.923±0.009	TNDCN	0.774±0.038/ 0.726±0.022	TNDCN	0.689±0.021	TNDCN	0.769±0.023

\* Dominance-R and Dominance-E were done on RESISTANCE-1 and ELEA respectively. For Dominance-E, results on both PDom and RDom labels are reported.

**Table 2: Performance comparison on three tasks: detecting dominance, deception and nervousness.**

detection task. The diffusion weights have been normalized such

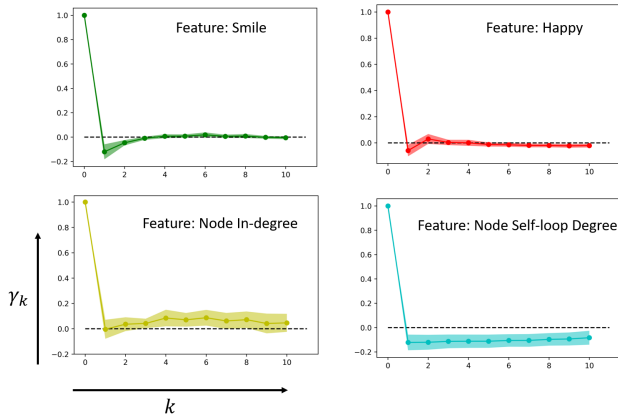


**Figure 4: Diffusion step weights of different features for the task of identifying the most nervous person in an interaction setting, 95% confidence interval shaded.**

that the 0-hop weight is 1. First, we observe that the 0-hop weight is significantly the largest, meaning that the original node features are very important to prediction. Therefore, the role of graph diffusion in this task can be roughly regarded as a fine-tuning process over the original features. Second, a clear contrast between the bottom two features is observed. While both of them can propagate quite long via the interactions, the way diffusion modifies the original features are quite different. We attribute such distinction to the two features' different real-world implications: node in-degree feature in a gazing network snapshot can be interpreted as the attention one received from other people at the corresponding moment, and thus indicates the interaction engagement level of that person. In contrast, the node self-loop feature can be interpreted as the probability that the person looked at his/her own screen at the corresponding moment, making the person look introverted and preservative. The different practical meanings entailed by the feature determines they are propagated via the interaction network in distinctive manners. Finally, the "smile" and "happy" emotion seem to be able to diffuse two steps while not beyond.

## 5.4 Ablation study

Ablation study on Task 1 is further conducted on RESISTANCE-1 to evaluate the usefulness of TNDCN building blocks independently.

No.	Replacement	Dominance
1	Original	0.923
2	S-TCN → LSTM	0.758
3	S-TCN → Mean Pooling	0.842
4	Diffusion → None	0.829
5	Diffusion → GCN-1*	0.844
6	Diffusion → GCN-2	0.889
7	Diffusion → GCN-4	0.784
8	Diffusion → GCN-6	0.701
9	Set $\beta = 1$	0.889

\* GCN for 1 layer, similar hereafter.

**Table 3: Ablation and comparison study with deception detection task (metric: Mean Accuracy).**

As shown by table 3, Eval. 2-3 further verify RNN's insufficiency on handling both extremely long time sequence and weak local dynamics. Interestingly, the very simple mean pooling can significantly outperform RNN and achieve close result even when compared with our set pooling technique. Eval. 4-8 focus on the graph-level techniques. Eval. 4 shows the importance of using network for prediction. Eval. 5-8 indicates the usability of GCN despite its serious decay because of over-smoothing and too many nonlinearities when going deep. In contrast, our network diffusion can propagate as long as 10 hops without significant decay in performance.

## 5.5 Further Scope Study

While we claim that TNDCN is especially helpful to deal with interaction sequences that are extremely long and high-frequent, one interesting question to ask is how it will perform if the sequence is relatively short and the dynamics are less frequent? We investigate this problem by further running TNGCN on CIAW [18], a dataset recording more than 92 people's timestamped proximities (of up to 1.2 meters) in a workplace over 20 days. The goal is to infer each person's department based solely on their interaction data. Notice that there is only one dynamic network, which we partition

into only 20 snapshots. Since no previous works were done on we focus on comparing with generic temporal GNN models. Please see supplementary material for more details of the settings and results. Our conclusion is that our model is still able to perform quite well even in this special scenario. We attribute this to the high flexibility of our S-TCN module to deal with sequences of various lengths.

## 6 CONCLUSION

In this work, we introduced a new neural-network-based representation learning model, TNDCN, which is particularly designed for dynamic social interaction networks. Dynamic social interaction networks contain highly dynamic node attributes with interactions with duration, which makes previous dynamic network embedding approaches not applicable. Our TNDCN model contains a network diffusion block that is capable of extracting patterns from complex interweaving of highly dynamic node attributes and interaction. It also leverages combination of TCN and set pooling that may learn the subtle and local patterns of social interactions randomly scattered in a long time span. TNDCN has been evaluated on three node-level prediction social tasks outperformed all previous baselines. The learned coefficients of TNDCN also give interesting social insights. Overall, TNDCN provides social scientists a powerful tool to automatically analyze social interactions to solve social tasks and extract knowledge for social science.

## REFERENCES

- [1] [n.d.].
- [2] Oya Aran and Daniel Gatica-Perez. 2013. One of a kind: Inferring personality impressions in meetings. In *Proceedings of the 15th ACM on International conference on multimodal interaction*. 11–18.
- [3] Siley O Ba and Jean-Marc Odobez. 2010. Multiperson visual focus of attention from head pose and meeting contextual cues. *IEEE Transactions on Pattern Analysis and Machine Intelligence* 33, 1 (2010), 101–116.
- [4] Chongyang Bai, Maksim Bolonkin, Judee Burgoon, Chao Chen, Norah Dunbar, Bharat Singh, VS Subrahmanian, and Zhe Wu. 2019. Automatic Long-Term Deception Detection in Group Interaction Videos. In *2019 IEEE International Conference on Multimedia and Expo (ICME)*. IEEE, 1600–1605.
- [5] Chongyang Bai, Maksim Bolonkin, Srijan Kumar, Jure Leskovec, Judee Burgoon, Norah Dunbar, and VS Subrahmanian. 2019. Predicting dominance in multiperson videos. In *Proceedings of the 28th International Joint Conference on Artificial Intelligence*. AAAI Press, 4643–4650.
- [6] Chongyang Bai, Srijan Kumar, Jure Leskovec, Miriam Metzger, Jay F. Nunamaker, and V. S. Subrahmanian. 2019. Predicting the Visual Focus of Attention in Multi-Person Discussion Videos. In *Proceedings of the Twenty-Eighth International Joint Conference on Artificial Intelligence, IJCAI-19*. International Joint Conferences on Artificial Intelligence Organization, 4504–4510. <https://doi.org/10.24963/ijcai.2019/626>
- [7] Tadas Baltrušaitis, Peter Robinson, and Louis-Philippe Morency. 2016. Openface: an open source facial behavior analysis toolkit. In *2016 IEEE Winter Conference on Applications of Computer Vision (WACV)*. IEEE, 1–10.
- [8] Cigdem Beyan, Francesca Capozzi, Cristina Becchio, and Vittorio Murino. 2017. Prediction of the leadership style of an emergent leader using audio and visual nonverbal features. *IEEE Transactions on Multimedia* 20, 2 (2017), 441–456.
- [9] Eunjoon Cho, Seth A Myers, and Jure Leskovec. 2011. Friendship and mobility: user movement in location-based social networks. In *Proceedings of the 17th ACM SIGKDD international conference on Knowledge discovery and data mining*. 1082–1090.
- [10] Fan Chung. 2007. The heat kernel as the pagerank of a graph. *Proceedings of the National Academy of Sciences* 104, 50 (2007), 19735–19740.
- [11] Hanjun Dai, Yichen Wang, Rakshit Trivedi, and Le Song. 2016. Deep coevolutionary network: Embedding user and item features for recommendation. *arXiv preprint arXiv:1609.03675* (2016).
- [12] Steven Davis and Paul Mermelstein. 1980. Comparison of parametric representations for monosyllabic word recognition in continuously spoken sentences. *IEEE transactions on acoustics, speech, and signal processing* 28, 4 (1980), 357–366.
- [13] Sergey Demyanov, James Bailey, Kotagiri Ramamohanarao, and Christopher Leckie. 2015. Detection of deception in the mafia party game. In *Proceedings of the 2015 ACM on International Conference on Multimodal Interaction*. 335–342.
- [14] Sergey Demyanov, James Bailey, Kotagiri Ramamohanarao, and Christopher Leckie. 2015. Detection of Deception in the Mafia Party Game. In *ACM ICMI*.
- [15] John F Dovidio and Steve L Ellyson. 1982. Decoding visual dominance: Attributions of power based on relative percentages of looking while speaking and looking while listening. *Social Psychology Quarterly* (1982), 106–113.
- [16] Nathan Eagle, Alex Sandy Pentland, and David Lazer. 2009. Inferring friendship network structure by using mobile phone data. *Proceedings of the national academy of sciences* 106, 36 (2009), 15274–15278.
- [17] Sergio Escalera, Xavier Baró, Jordi Vitria, Petia Radeva, and Bogdan Raducanu. 2012. Social network extraction and analysis based on multimodal dyadic interaction. *Sensors* 12, 2 (2012), 1702–1719.
- [18] Mathieu Génois, Christian L Vestergaard, Julie Fournet, André Panissov, Isabelle Bonmarin, and Alain Barrat. 2015. Data on face-to-face contacts in an office building suggest a low-cost vaccination strategy based on community linkers. *Network Science* 3, 3 (2015), 326–347.
- [19] G Giannakakis, Matthew Pedititis, Dimitris Manousos, Eleni Kazantzaki, Franco Chiarugi, Panagiotis G Simos, Kostas Marias, and Manolis Tsiknakis. 2017. Stress and anxiety detection using facial cues from videos. *Biomedical Signal Processing and Control* 31 (2017), 89–101.
- [20] Palash Goyal, Sujit Rokka Chhetri, and Arquimedes Canedo. 2020. dyngraph2vec: Capturing network dynamics using dynamic graph representation learning. *Knowledge-Based Systems* 187 (2020), 104816.
- [21] Ehsan Hajiramezani, Arman Hasanzadeh, Krishna Narayanan, Nick Duffield, Mingyuan Zhou, and Xiaoning Qian. 2019. Variational graph recurrent neural networks. In *Advances in Neural Information Processing Systems*. 10700–10710.
- [22] Dinesh Babu Jayagopi, Hayley Hung, Chuohao Yeo, and Daniel Gatica-Perez. 2009. Modeling dominance in group conversations using nonverbal activity cues. *IEEE Transactions on Audio, Speech, and Language Processing* 17, 3 (2009), 501–513.
- [23] Thomas N Kipf and Max Welling. 2016. Semi-supervised classification with graph convolutional networks. *arXiv preprint arXiv:1609.02907* (2016).
- [24] Johannes Klicpera, Aleksandar Bojchevski, and Stephan Günnemann. 2018. Predict then propagate: Graph neural networks meet personalized pagerank. *arXiv preprint arXiv:1810.05997* (2018).
- [25] David Lazer, Alex Pentland, Lada Adamic, Sinan Aral, Albert-László Barabási, Devon Brewer, Nicholas Christakis, Noshir Contractor, James Fowler, Myron Gutmann, et al. 2009. Computational social science. *Science* 323, 5915 (2009), 721–723.
- [26] Yaguang Li, Rose Yu, Cyrus Shahabi, and Yan Liu. 2017. Diffusion convolutional recurrent neural network: Data-driven traffic forecasting. *arXiv preprint arXiv:1707.01926* (2017).
- [27] Yozen Liu, Xiaolin Shi, Lucas Pierce, and Xiang Ren. 2019. Characterizing and Forecasting User Engagement with In-app Action Graph: A Case Study of Snapchat. In *Proceedings of the 25th ACM SIGKDD International Conference on Knowledge Discovery & Data Mining*. 2023–2031.
- [28] Franco Manessi, Alessandro Rozza, and Mario Manzo. 2020. Dynamic graph convolutional networks. *Pattern Recognition* 97 (2020), 107000.
- [29] Giang Hoang Nguyen, John Boaz Lee, Ryan A Rossi, Nesreen K Ahmed, Eunyee Koh, and Sungchul Kim. 2018. Continuous-time dynamic network embeddings. In *Companion Proceedings of the The Web Conference 2018*. 969–976.
- [30] Shogo Okada, Laurent Son Nguyen, Oya Aran, and Daniel Gatica-Perez. 2019. Modeling dyadic and group impressions with intermodal and interperson features. *ACM Transactions on Multimedia Computing, Communications, and Applications (TOMM)* 15, 1s (2019), 1–30.
- [31] Lawrence Page, Sergey Brin, Rajeev Motwani, and Terry Winograd. 1999. *The pagerank citation ranking: Bringing order to the web*. Technical Report. Stanford InfoLab.
- [32] Keith Rayner. 1998. Eye movements in reading and information processing: 20 years of research. *Psychological bulletin* 124, 3 (1998), 372.
- [33] Rudolph J Rummel. 1976. Understanding conflict and war: vol. 2: the conflict helix. *Bev-erly Hills: Sage* (1976).
- [34] Dairazalia Sanchez-Cortes, Oya Aran, Marianne Schmid Mast, and Daniel Gatica-Perez. 2011. A nonverbal behavior approach to identify emergent leaders in small groups. *IEEE Transactions on Multimedia* 14, 3 (2011), 816–832.
- [35] Aravind Sankar, Yanhong Wu, Liang Gou, Wei Zhang, and Hao Yang. 2020. DySAT: Deep Neural Representation Learning on Dynamic Graphs via Self-Attention Networks. In *Proceedings of the 13th International Conference on Web Search and Data Mining*. 519–527.
- [36] Atsushi Senju and Mark H Johnson. 2009. The eye contact effect: mechanisms and development. *Trends in cognitive sciences* 13, 3 (2009), 127–134.
- [37] Youngjoo Seo, Michaël Defferrard, Pierre Vandergheynst, and Xavier Bresson. 2018. Structured sequence modeling with graph convolutional recurrent networks. In *International Conference on Neural Information Processing*. Springer, 362–373.
- [38] Aymaz Taheri, Kevin Gimpel, and Tanya Berger-Wolf. 2019. Learning to Represent the Evolution of Dynamic Graphs with Recurrent Models. In *Companion Proceedings of The 2019 World Wide Web Conference*. 301–307.



- [39] Rakshit Trivedi, Mehrdad Farajtabar, Prasenjeet Biswal, and Hongyuan Zha. 2019. DyRep: Learning Representations over Dynamic Graphs. In *International Conference on Learning Representations*.
- [40] Petar Veličković, Guillem Cucurull, Arantxa Casanova, Adriana Romero, Pietro Lio, and Yoshua Bengio. 2017. Graph attention networks. *arXiv preprint arXiv:1710.10903* (2017).
- [41] Aldert Vrij. 2008. *Detecting lies and deceit: Pitfalls and opportunities*. John Wiley & Sons.
- [42] Fred O Walumbwa and John Schaubroeck. 2009. Leader personality traits and employee voice behavior: mediating roles of ethical leadership and work group psychological safety. *Journal of applied psychology* 94, 5 (2009), 1275.
- [43] Felix Wu, Tianyi Zhang, Amauri Holanda de Souza Jr, Christopher Fifty, Tao Yu, and Kilian Q Weinberger. 2019. Simplifying graph convolutional networks. *arXiv preprint arXiv:1902.07153* (2019).
- [44] Zhe Wu, Bharat Singh, Larry S Davis, and VS Subrahmanian. 2018. Deception detection in videos. In *Thirty-Second AAAI Conference on Artificial Intelligence*.
- [45] Bing Yu, Haoteng Yin, and Zhanxing Zhu. 2017. Spatio-temporal graph convolutional networks: A deep learning framework for traffic forecasting. *arXiv preprint arXiv:1709.04875* (2017).
- [46] Manzil Zaheer, Satwik Kottur, Siamak Ravanbakhsh, Barnabas Poczos, Russ R Salakhutdinov, and Alexander J Smola. 2017. Deep sets. In *Advances in neural information processing systems*. 3391–3401.
- [47] Lekui Zhou, Yang Yang, Xiang Ren, Fei Wu, and Yueting Zhuang. 2018. Dynamic network embedding by modeling triadic closure process. In *Thirty-Second AAAI Conference on Artificial Intelligence*.
- [48] Yuan Zuo, Guannan Liu, Hao Lin, Jia Guo, Xiaoqian Hu, and Junjie Wu. 2018. Embedding temporal network via neighborhood formation. In *Proceedings of the 24th ACM SIGKDD International Conference on Knowledge Discovery & Data Mining*. 2857–2866.